

The Papain Digestion of Skeletal Myosin A*

D. R. Kominz, E. R. Mitchell, T. Nihei, and C. M. Kay

ABSTRACT: Papain and insoluble cellulose-papain have been employed to digest myosin. The slow-sedimenting peak of papain-digested myosin is much larger than that of trypsin digests, indicating the presence of more than light meromyosin (LMM) in this peak. The papain heavy meromyosin (HMM) has a weight-average molecular weight between 115,000 and 140,000, indicating degradation to monomeric subfragments. A minor slow peak is present in papain HMM preparations, and the relative amount of the major fast peak is often diminished upon raising the pH or ionic strength. Ultraviolet optical rotatory dispersion measurements suggest that this process is accompanied by a loss of helical content. Possible explanations for the heterogeneity

of papain HMM in terms of dissociation of known myosin subunits or of isomerization of part of the fast peak are offered. Papain digestion in the presence of small concentrations of Ca^{2+} is reduced in extent, and results in the production of a multicomponent papain HMM. One of the components is a peak which, above a threshold level of pyrophosphate, responds to changes in Ca^{2+} concentration with alteration in sedimentation rate. It is proposed that this response is caused by change of swelling of the sensitive peak which is produced as a result of a specific crippling of the papain. The significance of this proposal for an entropic-osmotic mechanism of muscle contraction is briefly discussed.

The action of proteolytic enzymes such as trypsin and chymotrypsin on myosin involves a cleavage of the myosin molecule into two fragments (Perry, 1951; Gergely, 1953; Mihalyi and Szent-Gyorgyi, 1953). The smaller fragment, light meromyosin (LMM),¹ exhibits solubility characteristics similar to myosin. The larger fragment, heavy meromyosin (HMM), retains the adenosine triphosphatase (ATPase) activity of the parent molecule as well as its ability to combine with actin, and is soluble in low ionic strength solutions. Recently Mueller and Perry (1962) have demonstrated that further digestion of HMM with a high concentration of trypsin releases a smaller enzymatically active subfragment. While it is well established that papain splits γ -globulin into fragments retaining the ability to combine with antigen (Porter, 1958), the action of papain on myosin has not yet been reported.

A novel approach to the study of the action of enzymes on substrates has been introduced by Bar-Eli and Katchalski (1960), who have bound various enzymes to water-insoluble carriers through covalent linkages. The use of cellulose as a supporting medium

for insoluble enzymes was first described by Micheel and Ewers (1940), and the synthesis of various cellulose derivatives of trypsin and chymotrypsin was more recently reported by Mitz and Summari (1961). Such an insoluble derivative may readily be removed from the reaction mixture by either filtration or centrifugation, thereby terminating the reaction.

The present authors have observed that the digestion of myosin by papain or an insoluble complex of papain with carboxymethylcellulose results in the production of two fractions. One appears to be the same as LMM in terms of solubility characteristics. The other is similar to HMM both in solubility and in ATPase activity, while it is of smaller molecular weight. The latter fraction can exhibit a change in sedimentation pattern and in ultraviolet optical rotatory dispersion with varying ionic strength, suggesting that its conformation is dependent on the ionic environment. Moreover, certain preparations show a specific response to changes in Ca^{2+} concentration.

Experimental Procedures

Preparation of the Insoluble Papain Complex with Cellulose. The procedures recommended by Micheel and Ewers (1940) and Mitz and Summari (1961) were employed. Approximately 200 mg of crystalline papain suspension (Worthington Biochemical Corp.) was mixed with 750 mg of diazotized carboxymethylcellulose (Brown Co., Berlin, N. H.) in 120 ml of 0.075 M potassium phosphate buffer (pH 7.7), 5 mM cysteine, and 2 mM Versene. After stirring the mixture overnight at 5°, the insoluble cellulose complex was centrifuged down and washed with a solution containing 5 mM cysteine,

*From the National Institute of Arthritis and Metabolic Diseases, National Institutes of Health, Bethesda, Maryland, and the Department of Biochemistry, University of Alberta Medical School, Edmonton, Canada. Received April 21, 1965; revised June 3, 1965. This work was supported in part by research grants from the Canadian Muscular Dystrophy Association and from the National Institutes of Health, U. S. Public Health Service (AM-06287).

¹ Abbreviations used in this work: LMM, light meromyosin; HMM, heavy meromyosin; EGTA, ethylene glycol bis(β -aminoethyl ether)- N,N,N',N' -tetraacetic acid; ord, optical rotatory dispersion; ATPase, adenosine triphosphatase; BAEE, N -benzoyl-L-arginine ethyl ester.

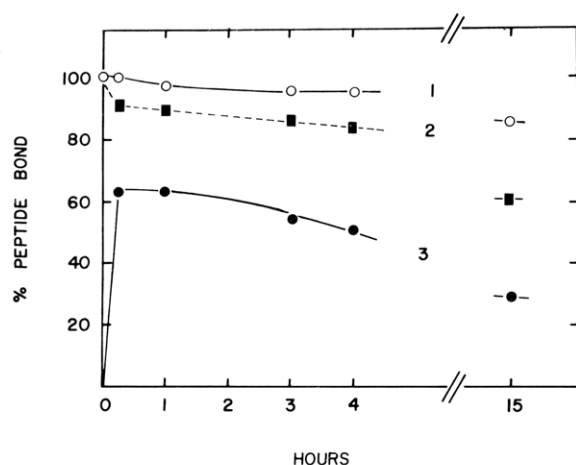


FIGURE 1: Time course of digestion of myosin with insoluble papain complex. Curve 1, reaction mixture; curve 2, total nondialyzable protein; curve 3, soluble nondialyzable protein. The reaction mixture contained 11.2 mg/ml of myosin in 0.5 M KCl, 0.05 M phosphate buffer, pH 7.0, 2 mM cysteine, and 0.3 mg/ml of papain as the insoluble complex.

2 mM Versene, and 0.01 M phosphate buffer, pH 7.5. The enzymatic activity of the papain-cellulose complex was assayed as described by Schwert and Takenaka (1955), employing as substrate 0.25 mM *N*-benzoyl-L-arginine ethyl ester (BAEE) in 0.067 M phosphate buffer, pH 6.9. The concentration of papain-cellulose was adjusted so that 0.2 ml of this suspension split 20 μ equiv of BAEE/min at 25°.

Preparation of Myosin A. Myosin A was extracted from rabbit skeletal muscle with 0.3 M KCl, 0.15 M phosphate buffer, pH 6.5, and purified by the method of Perry (1955) or of Kominz *et al.* (1959). Protein concentrations were determined by biuret color value, standardized by Kjeldahl nitrogen determinations. ATPase activity was determined at 25° in 0.1 M KCl, 10 mM CaCl_2 , 20 mM Tris-HCl buffer, pH 7.5, and 1 mM ATP. The inorganic phosphate liberated by the ATPase action was analyzed by the method of Fiske and Subbarow (1929) using trichloroacetic acid in a final concentration of 5% to deproteinize the reaction mixture.

Digestion of Myosin. The digestion of myosin A by papain-cellulose was initiated by adding 0.5 ml of the suspension of enzyme to 10 ml of about 1% myosin in 0.5 M KCl, 0.01 M phosphate buffer, pH 6.8. In addition 5 mM cysteine and 2 mM Versene were present in the reaction mixture as activators of papain. The reaction was terminated at various time intervals by centrifuging the reaction mixture at 3000 *g* for 2 min and separating the myosin digest from the papain-cellulose. The myosin digest was dialyzed overnight against ten volumes of 0.005 M phosphate buffer, pH 7.0. After removal of the precipitate, the supernatant was examined directly and alterations were made in the ionic strength and pH.

The digestion of myosin A by Ca^{2+} -weakened pa-

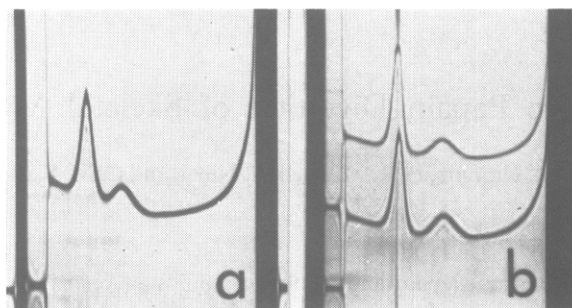


FIGURE 2: Sedimentation patterns of myosin digested with insoluble papain complex. (a) Digested 10 min at 25°; (b) digested 16 hr at 5° (top) and 2 hr at 23° (bottom). Solvent 0.5 M KCl and 0.05 M phosphate buffer; protein concentration 0.9–1.1%. Exposure in (a) made 66 min after reaching speed at bar angle of 50°; exposure in (b) made after 93 min at bar angle of 60°.

pain was carried out by adding Worthington papain to myosin in about a 300:1 substrate to enzyme ratio in the presence of 1 mM cysteine and 10^{-4} M Ca^{2+} . After digestion for 10 min at 22–25° in the pH-Stat at pH 7.4, the protein was quickly cooled and dialyzed against ten volumes of distilled water overnight. The precipitate was discarded, and the papain HMM supernatant was dialyzed against ten volumes of 0.01 M Tris buffer, pH 7.5, containing 1 mM pyrophosphate. The effect of adding Ca^{2+} , EGTA, Mg^{2+} , and pyrophosphate was examined in the ultracentrifuge.

Sedimentation Analyses. Sedimentation velocity experiments were performed in a Spinco Model E analytical ultracentrifuge with schlieren optics at a rotor speed of 59,780 rpm at 20°. In some of the sedimentation velocity studies, both a wedge-window cell and a plain-window cell were run simultaneously, giving two schlieren patterns in the same photographic frame. For molecular weight determinations, the Archibald method was employed in accordance with the procedures described by Schachman (1959). A speed of 9945 rpm was employed, and the temperature was maintained at 21° with the RTIC unit. Measurement of the concentration gradient at the cell bottom was facilitated by layering the protein solutions onto 0.1 ml of fluorocarbon, FC-43, supplied by Minnesota Mining and Manufacturing Co. The initial concentration of protein (c_0) in the cell was determined in arbitrary units by measuring the area of the boundary produced in a separate run at 59,780 rpm with the same solution and at the same bar angle (70°) as employed in the Archibald run. The c_0 values were corrected for radial dilution and extrapolated to zero centrifugation time. Measurement of the concentration gradients was performed as described in a previous publication (Kay *et al.*, 1961).

The molecular weight was also determined in a sedimentation equilibrium experiment utilizing the short-column technique with interference optics described by Richards and Schachman (1959). Three dilutions

were prepared of a sample which was over 95% fast component (see Figure 4a), dissolved in 0.04 M KCl, 0.0045 M phosphate buffer, pH 7.0. They were examined at 5563 rpm with the temperature held at 15°, using the four-place An-J rotor. The apparent molecular weight (M_{app}) of the major linear portion of the log c vs. x^2 plots was calculated from the formula $M_{app} = 2RT/[(d \ln c)/dx^2]/(1 - \bar{V}\rho)\omega^2$, and the weight-average molecular weight over the full length of the column was calculated as $M_w = 2RT(c_b - c_m)/[c_0(x_b^2 - x_m^2)/(1 - \bar{V}\rho)\omega^2]$. Determination of c_0 of the most concentrated solution was by an artificial boundary run at 5000 rpm.

Apparent Specific Volume Measurements. Densities of dialyzed protein solutions and their dialysates were determined with 10-ml capped pycnometers in a constant-temperature bath at 21.5°. Apparent specific volumes were calculated in accordance with the equation: $\phi' = (1/\rho_0) - (1/c)(\rho - \rho_0)/\rho_0$ where ρ_0 and ρ are the dialysate and solution densities, respectively, the c is the true protein concentration (g/ml), determined by the biuret method standardized against micro-Kjeldahl nitrogens, which, in turn, involved the figure of 16.3% as the nitrogen content of the protein.

Optical Rotatory Dispersion. The optical rotatory dispersion (ord) measurements were made in a Rudolph MSP-4 manual spectropolarimeter over the wavelength range of 220–300 m μ . The light source was an Osram XBO 450 w xenon lamp, and the cell path length employed was 0.01 dm. The double monochromator slit systems were all maintained at the same opening values and these were 0.3–0.4 mm at 233 m μ . A symmetrical angle of 2° was used throughout the measurements. The ord data have been evaluated, in terms of helical content based upon the magnitude of the rotation trough at 233 m μ in the ultraviolet region, as suggested by Simmons *et al.* (1961). The data were expressed in terms of $[m']\lambda$, defined as

$$[m']\lambda = [\alpha]\lambda \frac{\bar{M}}{100} \times \frac{3}{n^2 + 2}$$

where $[\alpha]\lambda$ is the specific rotation at wavelength λ , \bar{M} is the mean amino acid residue weight (taken here as 115), and n is the refractive index of the medium. In the calculation of $[m']\lambda$, a value of n at 265 m μ for H₂O (1.370) was used. The percentage helix was calculated from the size of the troughs on the assumption that there is a residue rotation difference at 233 m μ of approximately 13,000° between the α -helical and random conformations of the polypeptide chains (Blout *et al.*, 1962).

Results

After digestion was terminated by spinning down the papain-cellulose, the digest was dialyzed overnight against ten volumes of deionized water. As shown in Figure 1, curve 2, there was a 10% loss of peptide bond content following dialysis, indicating that digestion had liberated this much dialyzable peptide material. The

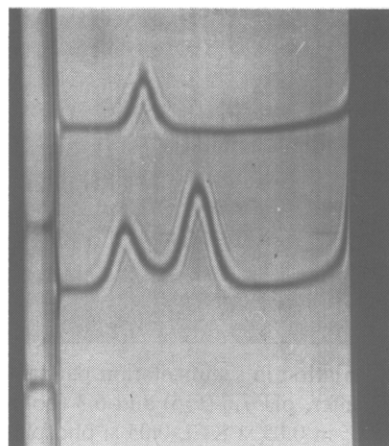


FIGURE 3: Sedimentation patterns of fractions of papain-digested myosin separated on the basis of solubility in 0.05 M KCl, 0.005 M phosphate buffer, pH 7.0. Top: insoluble fraction, redissolved in 0.3 M KCl, 0.09 M phosphate buffer, pH 7.0. Bottom: soluble fraction in 0.05 M KCl, 0.09 M phosphate buffer, pH 7.0. Exposure made after 90 min at bar angle of 50°.

portion of digested myosin remaining soluble at 0.05 ionic strength, hereafter referred to as papain HMM, amounted to approximately 65% of the protein initially present after 15 min of digestion (Figure 1, curve 3). With longer digestion some papain HMM is lost. The Ca²⁺-activated ATPase of papain HMM prepared by 15-min digestion was 12 ± 1 μ M inorganic phosphate/sec/g, which was 1.5 times the specific activity of myosin. Following 90-min digestion, there was 30% less activity than after 15 min of digestion.

Figure 2 illustrates the ultracentrifugal patterns of the entire reaction mixture at different times of papain digestion. A two-peak system is obtained with somewhat different features from that of myosin digested with trypsin. With 20 min of trypsin digestion at pH 7.0, the slower peak represents approximately 35% and the faster 60% of the combined areas (Mihalyi and Harrington, 1959); with 10 min of papain digestion, the proportion of the two peaks is reversed. Prolonged trypsin digestion causes alteration and diminution of the peaks; papain treatment of 2 to 16 hr brought about no change in the ratio of slow to fast component (Figure 2b). Digestion by trypsin at pH 8.1 for 8–20 min resembles the papain digestion in that the fast peak is reduced to 23%; however, at pH 8.1, the trypsin slow peak remains at 38% (Mihalyi and Harrington, 1959).

The fraction of papain-digested myosin which precipitated in 0.05 M KCl redissolved in 0.3 M KCl. It had similar sedimentation characteristics to those of trypsin LMM (Figure 3, top). Its ATPase activity was less than 5% of that of intact myosin.

The papain HMM fraction was unique in that its ultracentrifuge diagram consisted of two discrete peaks (Figure 3, bottom). Papain HMM from a large number

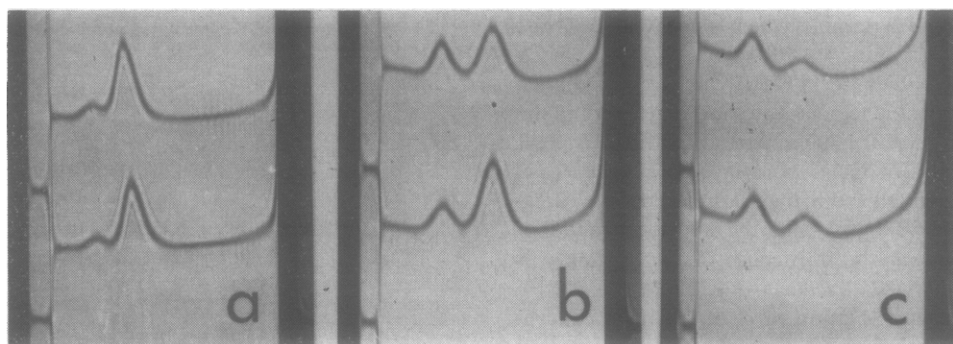


FIGURE 4: Variation in sedimentation patterns obtainable with papain HMM. (a) Preparation 8-2-3, 0.50% in 0.03 M phosphate buffer, pH 7.6 (top) and 6.3 (bottom). Exposure made after 50 min at bar angle of 50°. (b) Preparation 7-25-3, 0.63% in 0.05 M KCl, 0.05 M phosphate buffer, pH 7.6 (top) and 6.3 (bottom). Exposure made after 60 min at bar angle of 45°. (c) Preparation 6-23-3, 0.45% in 0.5 M KCl, 0.01 M phosphate buffer, pH 7.6 (top) and 6.3 (bottom). Exposure made after 76 min at bar angle of 45°. Preparation 8-2-3 was digested in the absence of added activator or buffer at a pH of approximately 6. Preparation 7-25-3 was digested in the presence of cysteine, EDTA, and phosphate buffer, pH 7. Preparation 6-23-3 was similarly prepared from myosin which has been stored in 50% glycerol for a number of months; the glycerol was removed by dialysis prior to digestion.

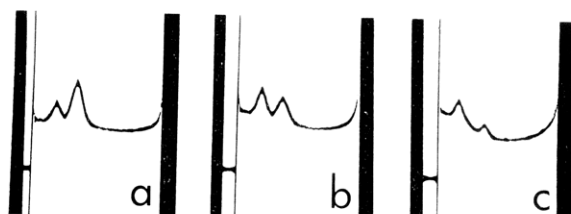


FIGURE 5: The effect of ionic strength on the sedimentation pattern of one preparation of papain HMM. (a) 0.05 M KCl; (b) 0.3 M KCl; (c) 0.6 M KCl. All solutions 0.65% protein and 0.01 M phosphate buffer, pH 7.0. Exposure made after 48 min at bar angle of 50°.

of different preparations was examined under varying conditions of ionic strength and pH, and in all cases the two peaks were present. The ratio of the areas under the two peaks varied from preparation to preparation; it also differed frequently in the same preparation under varying ionic and pH conditions (Figures 4 and 5). Higher pH or ionic strength in these cases decreased the amount of fast peak; sometimes this was accompanied by a proportionate increase in the amount of slow peak (Figure 4b), while sometimes there was no increase in slow peak but merely the appearance of low molecular weight substances which caused an elevation of the base line in the vicinity of the meniscus (Figure 5c). The intrinsic sedimentation coefficients, $S_{20,w}^0$, of the fast and slow components of papain HMM were evaluated from plots of $1/S_{20,w}$ vs. concentration and were found to be 5.4 S and 2.9 S, respectively (Figure 6).

Because the response of the ultracentrifuge pattern to changes of pH and ionic strength resembles an association-dissociation system, it was of interest to determine an average molecular weight of papain HMM under different conditions of ionic strength. The Archibald

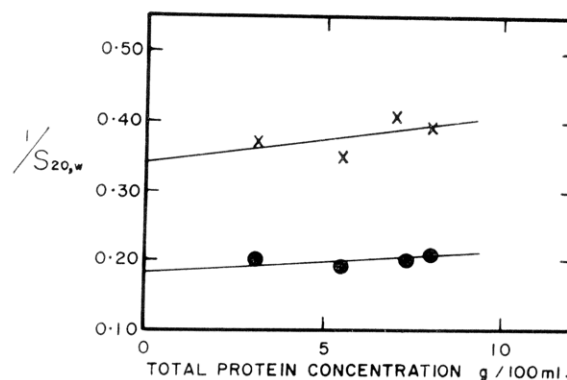


FIGURE 6: Concentration dependence of the reciprocal of the sedimentation rate of the two components of papain HMM. ●—●, fast component; ×—×, slow component.

bald approach to equilibrium was chosen for this purpose; it has been applied to interacting protein systems whose reactants and products had the same partial specific volume. The molecular weight of the papain HMM preparations of Figure 5 was determined at the two lower ionic strengths illustrated there: (a) 0.05 M KCl, 0.01 M phosphate, pH 7, where the fast component predominates; and (b) 0.3 M KCl, 0.01 M phosphate, pH 7, where the fast component is reduced and approximately equivalent to the slow one. For the calculation of molecular weights, the apparent specific volume was measured under both the above solvent conditions, and the results at several protein concentrations are listed in Table I. The data are seen to be invariant of both protein concentration and ionic strength, and ϕ' in either case was assigned a mean value of 0.75 ml/g.

The Archibald molecular weight values are sum-

TABLE I: Apparent Specific Volumes of Papain HMM (21°).

Solvent	Protein Concn (g/100 ml)	ϕ' (ml/g)
0.05 M KCl	0.72	0.748
	0.34	0.762
	0.21	0.753
0.3 M KCl	0.75	0.743
	0.38	0.754
Average: 0.752 ± 0.010		

marized in Table II. Although the papain HMM was heterogeneous, the weight-average molecular weight, \bar{M}_w , was essentially the same at both ionic strengths, approximately 140,000. Furthermore the \bar{M}_w values were independent of both cell position and time of measurement for any one experiment. It is apparent that we have been unable to detect any marked difference in molecular weight distribution either between the two samples or between top and bottom of the same sample.

There was evidence of heterogeneity in the $(d \ln c)/dx^2$ plots obtained by the sedimentation equilibrium procedure on the sample which was 95% fast component. The plots were linear over two-thirds of the fringes and then showed upward curvature. Both the M_{app} calculated from the linear portion of the plots and the M_w are plotted in Figure 7. Concentration dependence is slight, and both values appear to converge at an M_0 of about 115,000.

The possibility that conformational changes accompany the changes in sedimentation pattern illustrated in Figure 5 was investigated by ultraviolet

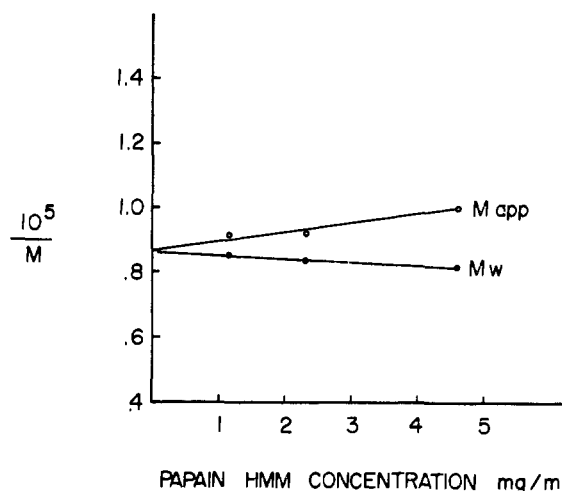


FIGURE 7: Concentration dependence of the reciprocal of the molecular weight of a preparation of papain HMM, determined by sedimentation equilibrium procedures. M_{app} , apparent molecular weight; M_w , weight-average molecular weight; calculated as described in text.

ord measurements. The sample of papain HMM, buffered by 0.01 M phosphate buffer, pH 7.0, was examined at 0.05 M KCl where the fast component predominated and at 0.5 M KCl where the fast component was sharply reduced. Figure 8 represents a plot of the effective residue rotation, $[m']$, as a function of wavelength. It is to be noted that the amplitude of the conformational Cotton effect at 233 $m\mu$ decreases as the ionic strength of the solvent system is increased. Assuming a residue rotation difference of 13,000° at $\lambda = 233 m\mu$ between the α -helical and random conformations of the polypeptide chain, values of 51.6 and 42.7% helix were

TABLE II: Molecular Weight of Papain HMM by Archibald Approach to Equilibrium Studies.

Solvent	Protein Concn (g/100 ml)	Time (min)	$\bar{M}_w \times 10^3$	
			Meniscus	Bottom
0.05 M KCl, 0.01 M phosphate, pH 7.0	0.72	16	143	126
		32	140	135
		48	142	141
		64	140	143
			Average: $138,000 \pm 5000$	
0.3 M KCl, 0.01 M phosphate, pH 7.0	0.53	16	130	128
		32	140	139
		48	134	139
		64	137	140
			Average: $135,000 \pm 5000$	
0.3 M KCl, 0.02 M phosphate, pH 7.2	0.35	32	138	140
		64	133	149
		98	140	147
			Average: $141,000 \pm 8000$	

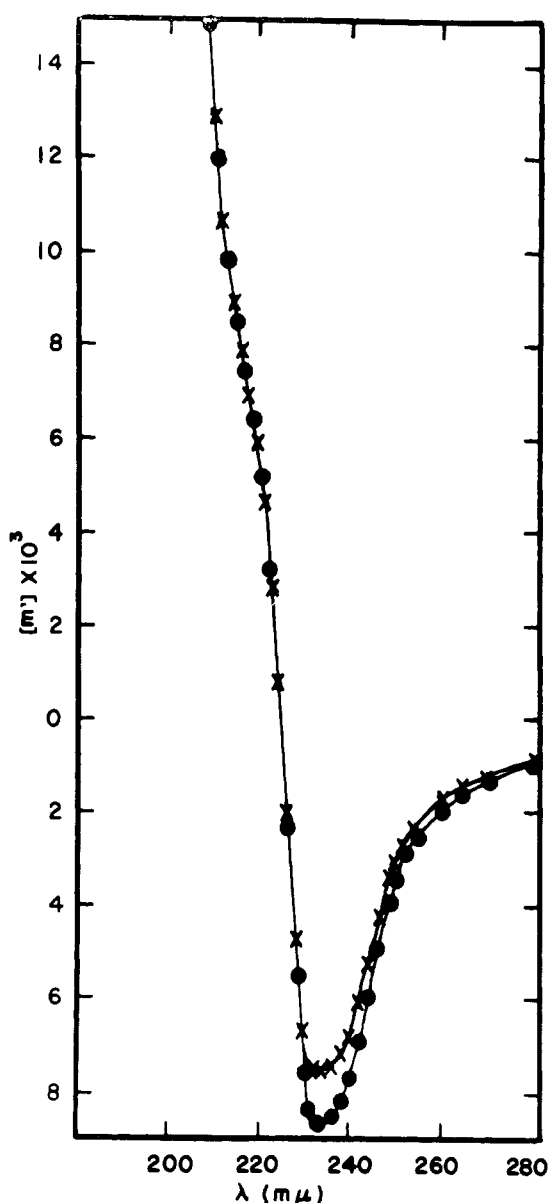


FIGURE 8: Wavelength dependence of effective residue rotation in the vicinity of the Cotton region at 233 $m\mu$. $\times - \times$, papain HMM in 0.5 M KCl, 0.01 M phosphate buffer, pH 7.0; $\bullet - \bullet$, papain HMM in 0.05 M KCl, 0.01 M phosphate buffer, pH 7.0.

interpolated for the papain HMM in 0.05 M KCl and 0.5 M KCl, respectively. This suggests that a decrease in α -helical content of papain HMM accompanies increase in ionic strength of the solvent.

Because of the evidence that small conformational changes of papain HMM could be accompanied by definite changes in ultracentrifuge pattern, investigations were undertaken into the effects of the specific binding agents, Ca^{2+} and ATP or pyrophosphate. These were routinely negative with papain HMM which had been digested in the presence of millimolar EDTA, and whose fast peak behaved as has hitherto

been described upon raising the pH. Material which had been digested in the presence of 10^{-4} M Ca^{2+} (or in one case by using very aged papain) behaved quite differently on raising the ionic strength. As shown in Figure 9c, top, raising the ionic strength causes the appearance of peaks of intermediate sedimentation rate between the fast and the slow peak. When such a multicomponent picture has been obtained by adding pyrophosphate, it has been readily reversed to the low ionic strength state by stirring the solution with some Dowex-1 chloride.

The effect of Ca^{2+} and EGTA on a preparation of multicomponent papain HMM is shown in Figure 9a. The bottom diagram is in the presence of 10^{-4} M Ca^{2+} ; the top diagram is in the presence of 10^{-5} M EGTA. A slower sedimenting portion of the fast peak is speeded up when the Ca^{2+} is removed. In the presence of 10^{-5} M Ca^{2+} , the same slower sedimenting portion of the fast peak is observed (Figure 9b, bottom); when this sample is made 10^{-4} M EGTA and 10^{-5} M Mg^{2+} , the slower sedimenting portion is again speeded up (Figure 9c, bottom). This suggests that Mg^{2+} cannot replace Ca^{2+} in causing the slowing of the sensitive portion of the fast peak. Figure 9d illustrates the same effect in a second preparation of papain HMM, where the sensitive peak sediments sufficiently slower than the fast peak so that its speed-up upon removal of Ca^{2+} does not cause overlap of the two peaks. Table III lists the sedimentation constants obtained from the ultracentrifuge diagrams; the final column compares the values for the sensitive peak in the presence and absence of Ca^{2+} . When the traces of Ca^{2+} normally present are removed by EGTA, the sensitive peak sediments 0.2 S faster; when 10^{-5} to 10^{-4} M Ca^{2+} is first added and then Ca^{2+} is removed by EGTA, an increase of 0.5 S takes place.

Although ATP is usually employed to study the relaxation-contraction response of muscle fibers or the clearing-superprecipitation phenomena of actomyosin systems, pyrophosphate also binds to myosin (Tonomura and Morita, 1959; Brahms and Brezner, 1961), causing shape change and dissociation of myosin B (Nihei and Tonomura, 1959). Therefore, in lieu of ATP whose concentration might be subject to change over the prolonged period of ultracentrifugation, pyrophosphate was employed in the studies of the effect of Ca^{2+} and EGTA on the multicomponent papain HMM. The pyrophosphate concentration in preparation I was not known because of the very slow penetration of polyanions through cellulose dialysis tubing at low ionic strength (Maruyama, 1962); the external concentration of pyrophosphate was 10^{-3} M. In the presence of 10^{-3} M Ca^{2+} , the sensitive peak is speeded up (Figure 9b, top). Since higher concentrations of pyrophosphate cause a remarkable slowing of the sensitive peak (Figure 9c, top), it was suspected that the anomalous speed-up caused by 10^{-3} M Ca^{2+} may have been due to its removing bound pyrophosphate from the protein of the sensitive peak. This view is supported by experiments performed on preparation IV of papain HMM, which was treated with Dowex-1 to remove any traces of polyanion and then a known amount of pyrophosphate

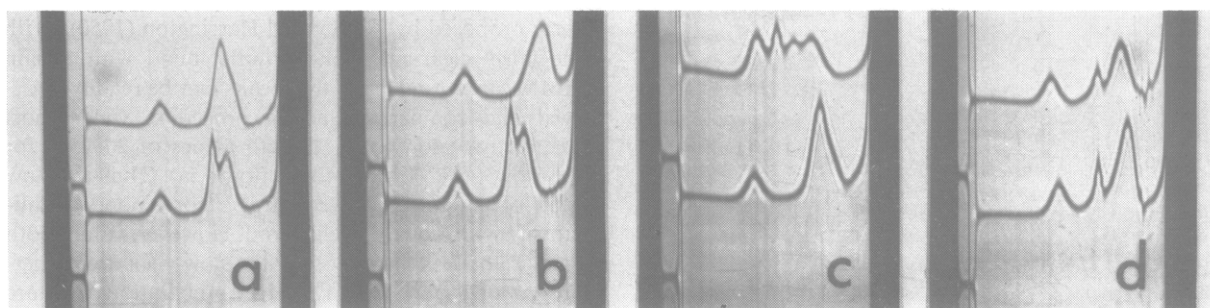


FIGURE 9: The response of multicomponent papain HMM to changes in concentration of Ca^{2+} and pyrophosphate. (a-c) Preparation I; (d) preparation IV. (a) (Bottom) 10^{-4} M Ca^{2+} , (top) 10^{-3} M EGTA; (b) (bottom) 10^{-5} M Ca^{2+} , (top) 10^{-3} M Ca^{2+} ; (c) (bottom) 10^{-5} M Ca^{2+} followed by 10^{-4} M EGTA + 10^{-5} M Mg^{2+} , (top) 10^{-2} M pyrophosphate; (d) (bottom) 10^{-4} M Ca^{2+} , (top) 10^{-4} M EGTA. Further description of conditions in text and Table III. Protein concentration 1.2%, temperature 15° . Exposure after 138 min at bar angle of 60° .

TABLE III: Effect of Specific Binding Agents on Sedimentation Rate of Multicomponent Papain HMM.

Multicomponent Papain HMM		Anions and Cations Added (M)				Sedimentation Rate (S)			
Preparation	Figure 9	Pyrophosphate	Ca^{2+}	EGTA	Mg^{2+}	Slow Peak	Fast Peak	Sensitive Peak	Δ
A. Effect of Removal of Ca^{2+}									
I	9a, bottom	$<10^{-3}$	10^{-4}	2.42	4.48	4.12	
I	9b, bottom	$<10^{-3}$	10^{-5}	2.49	4.63	4.23	
I	9a, top	$<10^{-3}$...	10^{-3}	...	2.52	4.5	4.36	0.13-0.24
I	9c, bottom	$<10^{-3}$	10^{-5}	10^{-4}	10^{-5}	2.55	4.67		0.44-0.55
I	...	$<10^{-3}$	10^{-4}	10^{-3}	...	2.52	4.67		0.44-0.55
B. Effect of Removal of Ca^{2+}									
IV	10^{-4}	2.52	4.57	3.84	
IV	10^{-4}	...	2.54	4.55	3.88	0.00
IV	9d, bottom	0.5×10^{-4}	10^{-4}	2.48	4.4	3.59	
IV	9d, top	0.5×10^{-4}	...	10^{-4}	...	2.42	4.4	3.77	0.18
C. Effect of Removal of Pyrophosphate									
I	9c, top	10^{-2}	10^{-3}	2.52	4.2, 3.7	3.15	
I	9b, top	$<10^{-3}$	10^{-3}	2.52	4.8		1.65

was added to it (Table III, part B). If no pyrophosphate was added, the sensitive peak showed no response to Ca^{2+} or EGTA, remaining at 3.86 S. In the presence of 0.5×10^{-4} M pyrophosphate 10^{-4} M Ca^{2+} slowed the sensitive peak to 3.6 S, and 10^{-4} M EGTA speeded it back to 3.8 S. Therefore it is confirmed that in the presence of Ca^{2+} , removal of pyrophosphate causes a speed-up of the sensitive peak. This experiment also demonstrates that a threshold concentration of pyrophosphate is required to allow the Ca^{2+} -EGTA antagonism to become evident.

An attempt was made to quantitate the effect of Ca^{2+} on papain by performing kinetic studies in the pH-Stat using 300:1 myosin to papain ratio. Assuming a pK at the pH 7.7-7.8 being maintained, we plot the number of peptide bonds split/ 10^5 g of protein against time of reaction in Figure 10. In the presence of 1 mM Ca^{2+} , the

rate was 70-80% of the rate in the presence of 1 mM EGTA; similar results were obtained using 10^{-5} - 10^{-3} M Ca^{2+} or 10^{-4} - 10^{-3} M EGTA. It thus appears that the specific lowered activity of papain indicated qualitatively in the sedimentation patterns of Figure 9 is illustrated quantitatively in the kinetic curves of Figure 10.

Discussion

At substrate to enzyme ratios of 250:1, trypsin digestion of myosin produces a HMM subunit of mol wt 340,000-400,000 (Holtzer *et al.*, 1962; Mueller, 1964; Young *et al.*, 1965). Further digestion with trypsin at substrate to enzyme ratios of 30:1 is required to produce the Mueller and Perry (1962) subfragment of mol wt 120,000 (Young *et al.*, 1965). The present results

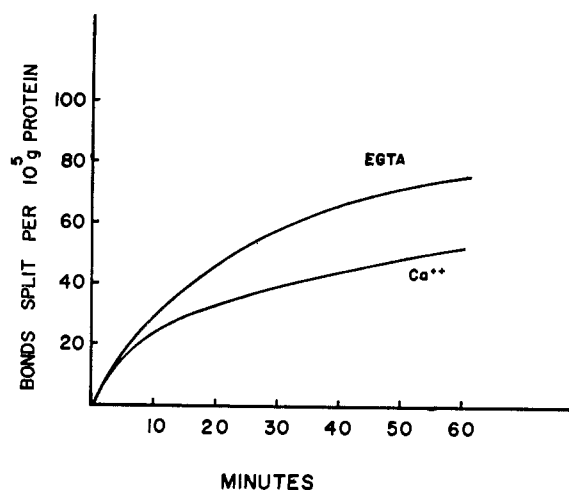


FIGURE 10: Kinetics of papain digestion of myosin in the presence or absence of Ca^{2+} at pH 7.7 and a temperature of 22–24°. 1 mM Ca^{2+} ; 1 mM EGTA.

indicate that in a single step at substrate to enzyme ratios of 300:1, papain can give monomeric HMM of about mol wt 120,000–140,000.

A second very obvious difference from the trypsin picture is the presence of two peaks with papain HMM. Lowey (1964) has reported that trypsin HMM splits at pH below 4 into two peaks whose $s_{20,w}^0$ are 3.3 and 10 S. Gel-filtration procedures allowed her to separate the slower sedimenting component; it had an α -helix content of 73% by optical rotatory dispersion, and an amino acid composition which strongly resembled that of LMM except in phenylalanine, methionine, and arginine. She identified it with the rodlike portion of HMM observed in electron micrographs (Rice, 1961). By varying pH and ionic strength she could change the relative proportions of the two peaks: raising the ionic strength caused the slow peak to emerge with the fast one due to a swamping-out of positive-charge repulsion, while lowering the ionic strength caused the fast peak to become polydisperse due to increased positive-charge repulsion.

The present results are comparable to Lowey's in several respects. The papain HMM slow peak has an $s_{20,w}^0$ of 2.9 S. Raising the ionic strength can cause the faster peak to become polydisperse because of increased negative-charge repulsion due to nonspecific anion binding (Figure 4c and 5c) or due to specific pyrophosphate anion binding (Figure 9c, top). There are also profound differences here from Lowey's findings. The fast peak's slower $s_{20,w}^0$ of 5.4 S reflects the low value of molecular weight of our preparation.

Lowey makes no estimate of the proportion of tryptic HMM that her 3.3S helical rod represents. Since Young *et al.* (1965) find that 80% of tryptic HMM is converted into the globulin subfragment, the helical rod would be expected to be found in the remaining 20%. If it constituted the entire 20%, the helical rod would have a molecular weight of 70,000–80,000 in the triple-stranded

form proposed by Kielley and Harrington (1960). With the fairly clear-cut peak patterns found with papain HMM, areas under the two peaks can be readily measured and compared. Such a procedure yields most frequently at low ionic strength values of 20–25% for the slow peak (Figure 4b, bottom; 5a). Thus the slow peak of papain HMM could also correspond quantitatively with Lowey's helical rod. However, values both greater and less than 20% for the slow peak are numerous among our papain HMM preparations (Figure 4a,b, top; 5b,c). An explanation for these departures is to be sought in the digestion conditions and in the ionic conditions of the solution being examined.

When high concentrations of papain (Figure 5) or aged preparations of myosin (Figure 4c) have been employed, the slow peak is approximately 20% at low ionic strength, and raising the ionic strength causes the fast peak to fragment as has already been described. When weak papain digestion mixtures are used a slow peak considerably less than 20% arises, and no change occurs on raising the pH or ionic strength (Figure 4a). When a papain digestion mixture of moderate strength is employed, the slow peak increases from about 20% at low ionic strength to about 30% at intermediate ionic strength or upon raising the pH from 6.3 to 7.6; no further change occurs with further increase in ionic strength. This shift in peak areas clearly illustrated in Figure 4b could have several explanations. One is that bound slow component is removed by the increased negative charge at higher pH. A second possibility is that LMM could be bound at low ionic strength and be released at high ionic strength; we have found this to occur with trypsin HMM. It may be pertinent that Noda and Ebashi (1960) found that in 0.2 M KCl myosin A is fully polymerized at pH 6.5 and fully dissociated at pH 7.3. A third explanation for the shift in peak areas is that isomerization of part of the 5.4S peak is occurring. Utilizing a molecular weight of 140,000 for each component, one can calculate the frictional ratios, f/f_0 , to be 1.64 and 3.04 for the fast and slow peaks, corresponding to anhydrous axial ratios of 12:1 and 56:1, or spherical swelling of 4.4 and 28, respectively. The occurrence of such large changes appears rather improbable.

When digestion has been performed with papain in the presence of Ca^{2+} , isomerization can be demonstrated in the ultracentrifuge patterns of papain HMM. It is clearly seen that the fast peak is composed of portions which respond to different extents when ionic conditions are changed, presumably because they have been degraded to different extents. Among these components of the fast peak is one, sharper and more responsive to ionic strength changes than the others, which has the capability of reacting sensitively to changes in Ca^{2+} concentration in the presence of optimum concentration of pyrophosphate.

Graded responses in sedimentation rate such as those given by the sensitive peak are more likely to result from changes in molecular shape rather than weight. Such shape changes can be considered as changes in axial ratio, in swelling, or in both param-

TABLE IV: Dependence of Sedimentation Rate of Papain HMM on Swelling When Axial Ratio Remains Constant.

Change in Sedimentation Δs_0	Frictional Ratio f/f_0^a	Maximum Swelling $(V_e/\bar{V})_{\max}$	Change in Maximum Swelling $\Delta(V_e/\bar{V})_{\max}$
0	1.64	4.4	
0.2	1.70	4.9	11%
0.5	1.81	5.95	35%

^a In calculating f/f_0 , the following values have been employed: $s_0 = 5.4$; $M_0 = 140,000$; $\bar{V} = 0.75$.

ters. HMM is 57% amorphous (Cohen and Szent-Gyorgyi, 1957), and its globular subfragment maintains this high amorphous content (Young *et al.*, 1965). Myosin possesses a swelling of 3.5 (Johnson and Rowe, 1961), and a large amount of swelling is also present in HMM. We are thus concerned with an amorphous swollen molecule, and the concepts of polymer chemistry are particularly applicable (Flory, 1953). Table IV lists the maximum change in swelling that would be represented by a change in sedimentation rate of a 5.4S molecule with 140,000 molecular weight. In the range of 0.2–0.5 Δs_0 encountered in the experiments with Ca^{2+} and EGTA in Table III there would be a maximum swelling of 11–35%.

In his pioneer experiments, Marsh (1952) found that in the presence of ATP muscle homogenates could swell 25%. Blum and Morales (1953) showed that ATP can induce a shape change in myosin B in solution. Recent evidence has pointed to a configurational change in myosin underlying the contractile process: Hoeve *et al.* (1963) have demonstrated a solvent- and temperature-dependent phase transition in glycerinated muscle fibers; Iyengar *et al.* (1964) have detected a transient hyperchromicity at 189 $m\mu$ upon addition of ATP to acto-HMM preparations. Although Hoeve *et al.* maintained that the entropic mechanism of Morales *et al.* (1955) was excluded by the demonstration of an essential phase change, the two processes are not mutually exclusive since a configurational change could trigger or accompany an entropic mechanism. Swelling indicated by osmotic effects and swelling indicated by hydrodynamic effects may be formally related to the same excluded volume (Flory, 1953). Assuming this, the evidence of the present work strongly suggests that the molecular site of the swelling found by Marsh is in the charge-sensitive globular subfragment of HMM.

Acknowledgments

The authors express their thanks to Miss B. Duntley,

Mr. J. Durgo, and Mr. K. Oikawa for their competent technical assistance.

References

- Bar-Eli, A., and Katchalski, E. (1960), *Nature* 188, 856.
 Blout, E. R., Schmier, I., and Simmons, N. S. (1962), *J. Am. Chem. Soc.* 84, 3193.
 Blum, J. J., and Morales, M. F. (1953), *Arch. Biochem. Biophys.* 43, 208.
 Brahms, J., and Brezner, J. (1961), *Arch. Biochem. Biophys.* 95, 219.
 Cohen, C., and Szent-Gyorgyi, A. G. (1957), *J. Am. Chem. Soc.* 79, 248.
 Fiske, C. H., and Subbarow, Y. (1929), *J. Biol. Chem.* 81, 629.
 Flory, P. J. (1953), *Principles of Polymer Chemistry*, Ithaca, N. Y., Cornell Univ. Press.
 Gergely, J. (1953), *J. Biol. Chem.* 200, 543.
 Hoeve, C. A. J., Willis, Y. A., and Martin, D. J. (1963), *Biochemistry* 2, 282.
 Holtzer, A., Lowey, S., and Schuster, T. M. (1962), *The Molecular Basis of Neoplasia*, Austin, Univ. of Texas Press, p. 259.
 Iyengar, M. R., Glauser, S. C., and Davies, R. E. (1964), *Biochem. Biophys. Res. Commun.* 16, 379.
 Johnson, P., and Rowe, A. J. (1961), *Biochim. Biophys. Acta* 53, 343.
 Kay, C. M., Smillie, L. B., and Hilderman, F. A. (1961), *J. Biol. Chem.* 236, 118.
 Kielley, W. W., and Harrington, W. F. (1960), *Biochim. Biophys. Acta* 41, 401.
 Kominz, D. R., Carroll, W. R., Smith, E. N., and Mitchell, E. R. (1959), *Arch. Biochem. Biophys.* 79, 191.
 Lowey, S. (1964), *Science* 145, 3632.
 Marsh, B. B. (1952), *Biochim. Biophys. Acta* 9, 247.
 Maruyama, K. (1962), *Sci. Papers College Gen. Educ., Univ. Tokyo* 12, 73.
 Micheel, F., and Ewers, J. (1940), *Makromol. Chem.* 31, 200.
 Mihalyi, E., and Harrington, W. F. (1959), *Biochim. Biophys. Acta* 36, 447.
 Mihalyi, E., and Szent-Gyorgyi, A. G. (1953), *J. Biol. Chem.* 201, 189.
 Mitz, M., and Summari, S. (1961), *Nature* 189, 576.
 Morales, M. F., Botts, J., Blum, J. J., and Hill, T. L. (1955), *Physiol. Rev.* 35, 475.
 Mueller, H. (1964), *J. Biol. Chem.* 239, 797.
 Mueller, H., and Perry, S. V. (1962), *Biochem. J.* 85, 431.
 Nihei, T., and Tonomura, Y. (1959), *J. Biochem. (Tokyo)* 46, 1355.
 Noda, H., and Ebashi, S. (1960), *Biochim. Biophys. Acta* 41, 386.
 Perry, S. V. (1951), *Biochem. J.* 48, 257.
 Perry, S. V. (1955), *Methods Enzymol.* 4, 32.
 Porter, R. R. (1958), *Nature* 182, 670.
 Rice, R. V. (1961), *Biochim. Biophys. Acta* 53, 29.
 Richards, E. G., and Schachman, H. K. (1959), *J. Phys. Chem.* 63, 1578.
 Schachman, H. K. (1959), *Ultracentrifugation in Bio-*

- chemistry, New York, Academic, p. 181.
- Schwert, G. W., and Takenaka, Y. (1955), *Biochim. Biophys. Acta* 16, 570.
- Simmons, N. S., Cohen, C., Szent-Gyorgyi, A. G., Wetlaufer, D. B., and Blout, E. R. (1961), *J. Am. Chem. Soc.* 83, 4766.
- Tomomura, Y., and Morita, F. (1959), *J. Biochem. (Tokyo)* 46, 1367.
- Young, D. M., Himmelfarb, S., and Harrington, W. F. (1965), *J. Biol. Chem.* 240, 2428.

Nuclear Magnetic Resonance Studies of Cytochrome *c*. Possible Electron Delocalization*

Arthur Kowalsky†

ABSTRACT: New resonances at abnormally high and low fields have been observed in the proton magnetic resonance spectrum of horse heart ferricytochrome *c*. They are not found in the spectrum of the reduced protein, nor are they found in the spectrum of the oxidized form either in 8 M urea or in acid solution. There are about four protons involved in each low-field resonance. These resonances have been used to estimate the rate of electron exchange between oxidized and reduced cytochrome *c*. Similar absorptions have been found in the spectra of cytochrome *c* of other species, of myoglobin, of the heme peptides, and of the hematin of cytochrome *c*. A comparison of the complete nuclear magnetic resonance spectrum of oxidized and reduced heme peptides indicates that the anomalous

resonances of these compounds may arise from the methine bridge protons of the porphyrin ring. Other possible partial sources are the ethyl and methylene protons immediately adjacent to the porphyrin ring and the protons α to carboxyl and amino groups. However, it does not seem likely that the contact resonances of the peptides are the same as those of ferricytochrome *c*.

The abnormal resonances may be the result of electron delocalization with consequent hyperfine contact interaction between the electron and certain protons of the heme or of the protein. They may also result from a pseudo-contact interaction. In view of the simplicity of the protein contact spectra, the latter interaction does not seem likely.

The proton magnetic resonance spectra of proteins consist of a series of broad absorptions whose total width covers a range of roughly 10 ppm (Kowalsky, 1962a; Bovey *et al.*, 1959). The shapes of these absorptions, of small molecular weight proteins, are characteristic of the composition of the protein (Jardetzky and Jardetzky, 1957) and also of the internal mobility or flexibility of the peptide chain (Kowalsky, 1962a). In this respect, differences observed between the spectra of the oxidized and reduced forms of cytochrome *c* have been attributed mainly to modifications in the conformation of the protein moiety with subsequent changes in the mobility of portions of the peptide chain. The electronic effect, *i.e.*, the influence of an unpaired electron on the spectra of a previously diamagnetic species, was assumed to be small. Recent experiments in some small

organic paramagnetic complexes (Eaton *et al.*, 1962) have pointed up the fact that, in such systems, the electronic effect is far from negligible. Indeed, new resonances, far removed from the normal range, have now been found in the spectrum of oxidized cytochrome *c* which are definitely and intimately related to the presence of the paramagnetic metal ion. This paper is a report of investigations concerned with these new resonances, the conditions of their appearance, their source, and other information which can be derived from measurements on them. These new resonances will be referred to as "contact resonances," and a distinction between the two possible types of contact resonance will be made in the discussion.

Experimental Section

Materials. Cytochrome *c*, type III from horse heart, was obtained from Sigma Chemical Co. Various lot numbers were used. The product usually contained some reduced form. Completely oxidized cytochrome *c* was obtained by treating the commercial material with the minimum amount of potassium ferricyanide. The

* From the Johnson Research Foundation, University of Pennsylvania, Philadelphia, Pa. Received April 24, 1965. This work was supported by U. S. Public Health grants (AM-06940 and GM-12446). A preliminary report of this paper has been presented (Kowalsky, 1964).

† Research Career Development Awardee, U. S. Public Health Service.